GEOSABERES: Revista de Estudos Geoeducacionais
ISSN: 2178-0463
fabiomoria@gmail.com
Universidade Federal do Ceará
Brasil

INTRODUCING THE MAIN AND ACCESSORY MINERALS IN THE GRANITOID BATHOLITH OF SHIRKUH, YAZD (CENTRAL IRAN) AND ITS TOURMALINE AND GARNET PHASES

Az-Mikaelians, Hripsimeh; Ashja-Ardalan, Afshin; Sheikhzakariayi, Seyed-Jamal; Ansri, Shiva
INTRODUCING THE MAIN AND ACCESSORY MINERALS IN THE GRANITOID BATHOLITH OF SHIRKUH, YAZD (CENTRAL IRAN) AND ITS TOURMALINE AND GARNET PHASES
GEOSABERES: Revista de Estudos Geoeducacionais, vol. 11, 2020
Universidade Federal do Ceará, Brasil
Available in: https://www.redalyc.org/articulo.oa?id=552861694058
DOI: https://doi.org/10.26895/geosaberes.v11i0.910

INTRODUCING THE MAIN AND ACCESSORY MINERALS IN THE GRANITOID BATHOLITH OF SHIRKUH, YAZD (CENTRAL IRAN) AND ITS TOURMALINE AND GARNET PHASES

APRESENTANDO OS MINERAIS PRINCIPAIS E ACESSÓRIOS NO BATÓLITO GRANITÓIDE DE SHIRKUH, YAZD (IRÃ CENTRAL) E SUAS FASES DE TURMALINA E GRANADA

PRESENTANDO LOS MINERALES PRINCIPALES Y ACCESORIOS EN EL BAUTISMO GRANITOIDE DE SHIRKUH, YAZD (IRÁN CENTRAL) Y SUS FASES DE TURMALINA Y GRANATE

Hripsimeh Az-Mikaelians
Islamic Azad University, Irán
ripsy_567@yahoo.com
https://orcid.org/0000-0003-3772-2974

Afshin Ashja-Ardalan
Islamic Azad University,, Irán
afshinashjaardalan@yahoo.com
https://orcid.org/0000-0002-1800-9594

Seyed-Jamal Sheikhzakariayi
Islamic Azad University, Irán
j.sheikhzakaria@gmail.com
https://orcid.org/0000-0002-4288-572X

Shiva Ansri
Islamic Azad University, Irán
ansari@iiau.ac.ir
https://orcid.org/0000-0001-7539-1892

DOI: https://doi.org/10.26895/geosaberes.v11i0.910
Redalyc: https://www.redalyc.org/articulo.oa?id=552861694058

Received: 01 October 2019
Accepted: 13 December 2019
Published: 10 January 2020

Abstract:

Batholith of Shirkuh, Yazd, is part of the central Iranian structural zone, located southwest of the province. The batholith is composed of five rock units, namely monzogranite, granodiorite, quartz monzonite, quartz monzodiorite, and syenogranite.The batholith, having cut through the Nayband formation (Upper Triassic), with Cretaceous limestones and a sandstone and conglomerate unit (Lower Cretaceous) lying on top as an angular unconformity, probably dates back to the Jurassic. Field and experimental investigations revealed various accessory minerals in the granite mass, including garnet, tourmaline, amphibole, zircon, sphene, apatite, biotite, muscovite, and epidote. The garnet, tourmaline, and amphibole were investigated by an Electron Microprobe (EMP), revealing the granite mass to be of almandine, grossular, and uvarovite types, the tourmaline of the rossmanite and foitite types, and amphiboles of the tschermakite and hornblende types.

Keywords: Garnet, Tourmaline, Shirkuh Granite, Iran, Yazd.

Resumo:

O batólito de Shirkuh, Yazd, faz parte da zona estrutural central do Irã, localizada a sudoeste da província. O batólito é composto por cinco unidades de rochas, a saber monzogranito, granodiorito, quartzo monzonito, quartzo monzodiorito e sienogranito. O batólito, após cortar a formação de bandas nay (Triássico Superior), possui calcários cretáceos e uma unidade de arenito e conglomerado (Cretáceo Inferior). deitado no topo como uma inconformidade angular, provavelmente remonta ao Jurássico. Investigações experimentais e de campo revelaram vários minerais acessórios na massa de granito, incluindo granada, turmalina, anfibólio, zircão, esfeno, apatita, biotita, moscovita e epídoto. A granada, a turmalina e os anfibólios foram investigados por um

Electron Microprobe (EMP), revelando que a massa de granito era do tipo almandina, grossular e uvarovita, a turmalina do tipo rossmanita e foitita e anfibólios dos tipos tschermakita e hornblenda.

Palavras-chave: Granada, Turmalina, Granito Shirkuh, Irã, Yazd.

Resumen:

Batholith de Shirkuh, Yazd, es parte de la zona estructural central iraní, ubicada al suroeste de la provincia. El batolito se compone de cinco unidades de roca, a saber, monzogranita, granodiorita, monzonita de cuarzo, monzodiorita de cuarzo y sinoenogranita. El batolito, que ha atravesado la formación Nayband (Triásico Superior), con calizas cretáceas y una unidad de arenisca y conglomerado (Cretácico Inferior) acostado en la parte superior como una disconformidad angular, probablemente se remonta al Jurásico. Las investigaciones de campo y experimentales revelaron varios minerales accesorios en la masa de granito, incluyendo granate, turmalina, anfíbol, circonio, esfeno, apatita, biotita, moscovita y epidota. El granate, la turmalina y el anfíbol fueron investigados por un Microprobe de electrones (EMP), revelando que la masa de granito era de tipo almandino, grosular y uvarovita, la turmalina de los tipos rossmanita y foitita, y anfíboles de los tipos tschermakita y hornblende.

Palabras clave: Granate, Turmalina, Granito Shirkuh, Irán, Yazd.

INTRODUCTION

Parte The Electron Microprobe (EMP) is a major contributor to progress in petrology, as a field of science, and can provide significant help in identifying rock formations and determining the temperature and pressure conditions of intrusive rocks. Further, other applications of this method include the accurate identification of minerals, particularly those in the solid solution series. An example is the precise naming of the type of plagioclases, amphiboles, garnets, and tourmalines in the plutonic rocks of the region.

RESEARCH METHOD

In this study, samples of various rock compositions were collected for a mineralogy study of the thin sections to investigate the geochemistry of accessory minerals in granitoid batholith of Shirkuh, Yazd. The samples were delivered to Zarazma Mineral Studies Co. for chemical XRF and ICP–MS analysis (Table 1 and 2). Then, some of the detectable main and accessory minerals were submitted to Kansaran Binaloud Co. for EMP analysis.

Table 1 - Chemical analysis of the Yazd granitoid rock mass by the XRF method

Sample	Importar imagen	Importar imagen	Importar imagen	Importar imagen	Importar imagen	Importar imagen	Importar imagen	Importar imagen	Importar imagen	Importar imagen	Importar imagen	Importar imagen	Importar imagen	Importar imagen
Importar imagen	0.05	0.05	0.05	0.05	0.05	0.05	0.05	0.05	0.05	0.05	0.05	0.05	0.05	0.05
H1	70.52	13.84	<	2.48	4.20	3.46	1.33	0.09	2.55	0.13	<	0.51	0.90	100
H2	70.46	14.47	0.05	2.01	3.49	4.2	1.04	0.06	2.59	0.11	<	0.45	1.07	100
H13	60.43	17.56	0.06	4.94	6.24	3.32	2.23	0.15	3.18	0.26	<	0.65	0.98	100
H16	69.81	14.64	<	2.13	3.87	3.81	1.24	0.08	2.53	0.13	<	0.47	1.28	99.99
H20	72.02	14.91	<	3.47	1.78	0.71	1.31	<	3.64	0.12	<	0.41	1.63	100
H27	67.78	15.33	0.05	2.81	4.49	3.7	1.23	0.09	2.72	0.14	<	0.55	1.13	100
H31	69.38	14.14	<	2.39	4.39	3.52	1.25	0.10	2.75	0.14	<	0.55	1.37	99.98
H35	68.70	13.95	<	2.53	4.66	3.22	1.54	0.10	2.85	0.13	<	0.54	1.77	99.99
H39	64.34	16.51	<	1.86	5.04	0.49	1.76	0.14	7.17	0.19	<	0.69	1.80	99.99
H43	71.97	13.25	<	1.99	2.25	4.43	0.74	0.08	2.69	0.13	<	0.28	2.19	100
H46	69.01	14.53	0.05	2.35	4.25	3.72	1.08	0.09	2.7	0.14	<	0.5	1.56	99.98
H49	71.07	14.13	<	2.28	3.90	3.51	1.05	0.08	2.71	0.13	<	0.48	0.66	100
H50	60	21.78	<	2.9	1.41	2.4	1.27	<	7.1	0.18	<	0.61	2.37	100
H55	69.35	14.75	<	2.31	4.40	3.55	1.27	0.08	2.60	0.14	<	0.53	1.02	100
H58	67.81	15.49	0.06	2.64	4.23	3.93	1.02	0.1	2.93	0.24	<	0.49	1.07	100
H64	70.48	14.42	<	2.04	3.64	3.83	1.03	0.07	2.76	0.13	<	0.46	1.14	100
H66	70.78	13.77	<	1.90	4.02	3.81	1.17	0.08	2.72	0.14	<	0.49	1.13	100
H70	67.68	15.5	0.06	2.19	4.58	3.77	1.24	0.1	2.86	0.15	<	0.56	1.29	99.98
H71	68.38	15.36	0.06	1.96	3.47	4.13	1.05	0.07	3	0.12	<	0.42	1.98	100
H73	64.28	16.46	0.06	3.59	5.7	2.83	1.66	0.11	2.84	0.14	<	0.72	1.6	99.99
H75	66.46	15.59	0.06	2.57	4.53	3.4	1.31	0.1	3.02	0.15	<	0.54	2.26	99.99
H76	70.30	13.68	<	1.64	4.14	3.18	1.37	0.09	3.01	0.13	<	0.48	1.98	100
H81	67.73	15.05	0.06	1.42	4.49	4.51	1.28	0.09	2.52	0.14	<	0.54	2.18	100
H83	73.46	13.00	<	0.98	2.11	4.58	0.62	0.05	2.80	0.11	<	0.22	2.08	100
H84	73.63	13.45	<	1.17	2.06	4.42	0.68	0.06	2.69	0.12	<	0.25	1.46	99.99
H88	70.98	13.77	0.05	2.80	3.02	3.91	1.16	0.08	3.39	0.10	<	0.41	0.34	100
H91	69.14	14.98	0.07	2.87	3.12	4	1.03	0.07	3.69	0.09	<	0.4	0.53	100
H95	55.59	17.29	0.05	6.92	7.59	2.25	3.72	0.25	3.92	0.2	<	0.92	1.3	99.99
H96	62.69	16.15	0.06	4.25	5.8	3.36	2.27	0.17	3.49	0.16	<	0.7	0.91	100
H97	69.78	14.82	0.08	2.83	3.06	4.16	1.02	0.06	3.49	0.09	<	0.38	0.24	100

Table 2 - Chemical analysis of the Yazd granitoid rock mass by the ICP–MS method.

Sample	Ag	Al	As	Ba	Be	Bi	Ca	Cd	Ce	Co	Cr	Cs	Cu	Dy
Importar imagen	0.1	100	0.1	1	0.2	0.1	100	0.1	0.5	1	1	0.5	1	0.02
H1	0.1 <	77887	6.7	442	2.5	0.2	18058	0.1 <	82	10.6	44	10.6	19	4.8
H2	2.8	67689	5.7	383	1.8	0.2	13815	0.1 <	72	7.6	23	8.6	11	4.18
H13	0.6	80142	0.1 <	444	2.1	0.2	33009	0.1	51	12.8	23	13.6	29	2.63
H16	0.1 <	76274	1.3	450	2.8	0.2	15654	0.1 <	78	9.4	42	9	45	4.96
H20	0.1 <	79538	3.5	106	3.2	0.2	26584	0.1	74	5.6	30	3.1	5	5.44
H27	0.4	73798	9.4	358	2.4	0.2	19513	0.1	67	10.1	27	8.8	21	4.42
H31	0.1 <	78776	7.7	501	2.3	0.2	17563	0.1	88	10.5	45	7.7	16	4.74
H35	0.1 <	83920	11.8	478	2.5	0.2	20532	0.1	86	10.2	47	5.1	22	4.53
H39	0.1 <	91933	2.9	78	4.2	0.3	14298	0.1 <	80	14.1	58	0.5 <	11	6.66
H43	0.1 <	71993	3.8	306	2.4	0.2	14556	0.1 <	52	4.8	26	5.3	10	4.22
H46	2.1	71600	5	389	2.4	0.2	17255	0.1 <	70	9.4	26	5.6	21	4.96
H49	0.1 <	82152	2.9	481	2.9	0.2	18649	0.1 <	87	9.6	42	8.3	17	4.06
H50	5.1	96825	3	274	3.4	0.3	20625	0.1	26	3.5	21	8.6	12	2.96
H55	0.1 <	84657	8.5	472	2.7	0.2	18677	0.1	92	10.6	46	12.3	16	4.33
H58	3.5	72554	7.2	445	2	0.3	16866	0.1 <	70	8.4	28	7.8	16	4.88
H64	0.1 <	79838	4.5	508	2.6	0.2	15255	0.1	83	8.6	32	9.3	15	4.28
H66	0.1 <	72822	6.2	497	2.7	0.2	14301	0.1 <	83	9	40	8.9	18	4.43
H70	3	72864	0.9	437	1.9	0.2	14760	0.1	69	9.2	57	9.6	7	3.78
H71	0.1 <	71081	1.5	431	1.6	0.2	13212	0.1 <	65	6.2	92	3.1	7	5.3
H73	0.1 <	77608	4.8	454	107	0.2	25415	0.1 <	85	12.9	79	2.6	18	4.96
H75	0.2	74229	11.1	382	2.2	0.4	17050	0.1 <	74	9.5	52	3.6	10	4.62
H76	0.1 <	78267	4.6	472	2.4	0.2	12552	0.2	87	9.9	48	3.6	6	5.03
H81	0.4	67540	3.8	432	2.4	0.2	9328	0.1	59	8.3	38	10.8	9	4.2
H83	0.1 <	72722	9.2	343	2.5	0.4	7282	0.5	49	2.4	20	6.4	18	2.97
H84	0.1 <	76374	8.6	320	2.7	0.5	8888	0.1	59	4.1	28	10	21	4.14
H88	0.1 <	73345	0.1 <	607	1.8	0.2	20057	0.1 <	59	6.9	15	2.5	9	3.86
H91	0.3	63763	0.1 <	487	2	0.2	18326	0.1 <	60	6	12	4.4	6	3.73
H95	0.1 <	81973	0.1 <	335	3.7	0.3	45425	0.1 <	65	17.1	19	8.4	26	9.61
H96	0.1 <	74228	0.1 <	409	2.7	0.2	28466	0.1	62	12.6	37	5.7	21	6.19
H97	0.1 <	68604	0.1 <	520	1.3	1.1	19076	0.1 <	51	5.8	22	2.6	82	2.94

Table 2 (cont.)

Sample	Er	Eu	Fe	Gd	Hf	In	K	La	Li	Lu	Mg	Mn	Mo	Na
Importar imagen	0.05	0.1	100	0.05	0.5	0.5	100	1	1	0.1	100	5	0.1	100
H1	2.21	1.02	33477	4.85	0.5 <	0.5 <	30288	43	79	0.27	8620	773	0.1	23568
H2	1.8	0.83	24356	5.61	2.18	0.5 <	33721	34	59	0.26	6173	400	0.1 <	19600
H13	1.29	1.28	39933	3.32	0.78	0.5 <	26959	27	61	0.18	12063	986	0.1 <	23176
H16	2.41	1.04	31377	5.05	0.5 <	0.5 <	31645	41	83	0.3	8338	663	0.1	22096
H20	2.66	0.96	17194	4.95	0.5 <	0.5 <	5743	38	32	0.32	8595	195	0.1 <	31783
H27	2.04	1.03	30948	5.31	0.75	0.5 <	29341	33	69	0.24	7233	615	0.1 <	19882
H31	1.91	1.18	34223	5.5	0.5 <	0.5 <	29704	46	86	0.22	8170	765	0.4	24483
H35	1.82	1.24	35955	5.27	0.5 <	0.5 <	27601	46	78	0.21	9716	754	0.8	24477
H39	3.4	0.69	37225	5.9	0.5 <	0.5 <	3751	39	33	0.41	11180	1052	2.1	61928
H43	1.8	0.77	20244	4.02	0.53	0.5 <	31265	25	53	0.2	5078	614	10	23681
H46	2.42	1.01	30563	5.69	0.73	0.5 <	30106	35	71	0.31	6656	650	0.1 <	20216
H49	1.51	1.01	32644	4.95	0.5 <	0.5 <	31616	44	99	0.18	7300	666	21.8	25174
H50	1.23	1.05	10081	3.47	0.95	0.5 <	19395	11	32	0.13	7464	227	0.1 <	51237
H55	1.56	1.1	36006	5.24	0.5 <	0.5 <	32070	48	87	0.19	8679	661	20.2	24714
H58	2.55	1.02	27946	5.57	0.81	0.5 <	31882	34	77	0.33	5811	584	0.1 <	20218
H64	1.67	1.07	30075	5.02	0.5 <	0.5 <	33802	42	109	0.19	6921	600	10.1	24811
H66	1.85	0.94	31761	4.96	0.5 <	0.5 <	32827	40	64	0.22	7577	646	0.2	23669
H70	1.33	0.98	30120	5.2	0.59	0.5 <	31562	34	74	0.15	7145	612	0.1 <	20189
H71	2.6	0.89	24515	5.67	0.5 <	0.5 <	33720	33	52	0.27	6108	446	0.1 <	20248
H73	2.56	1.26	37261	6.13	0.5 <	0.5 <	24364	41	58	0.32	9384	743	0.1 <	20791
H75	2.18	0.98	29754	5.48	0.76	0.5 <	28095	37	69	0.28	7351	612	0.1 <	20544
H76	2.18	0.99	34563	5.46	0.5 <	0.5 <	27890	44	37	0.24	9340	701	0.1 <	26825
H81	2.2	0.79	28759	4.69	0.76	0.5 <	35322	29	54	0.29	7152	581	0.1 <	17261
H83	1.16	0.63	19044	3.09	0.5 <	0.5 <	38172	24	30	0.17	4166	400	0.1	24247
H84	1.51	0.9	20880	4.05	0.5 <	0.5 <	36257	29	33	0.19	4540	422	0.1 <	24062
H88	2.16	0.96	24983	3.37	0.5 <	0.5 <	31616	34	30	0.31	7453	582	0.4	27857
H91	2.31	0.71	20753	3.67	0.54	0.5 <	31573	32	30	0.38	5751	456	0.9	24228
H95	6.8	0.97	47759	8.78	1.43	0.5 <	19415	26	51	1.2	18384	1622	0.1 <	27679
H96	4.06	0.89	36804	6.12	0.98	0.5 <	26523	29	41	0.65	12208	1080	0.1	23849
H97	1.65	0.73	21064	3.04	0.76	0.5 <	33881	28	22	0.25	5831	398	0.1 <	23559

Table 2 (cont.)

Sample	Nb	Nd	Ni	P	Pb	Pr	Rb	S	Sb	Sc	Se	Sm	Sn	Sr
Importar imagen	1	0.5	1	10	1	0.05	1	50	0.5	0.5	0.5	0.02	0.1	1
H1	24	28.6	14	703	24	7.64	141	63	0.9	17.7	1.02	5.67	6	139
H2	14.8	33.1	16	491	35	8.73	164	56	0.8	10.3	6.75	6.66	3.8	83.6
H13	20.4	23.1	10	1151	33	6.01	145	93	0.9	9.3	2.9	4.17	3.5	392
H16	26.3	28.9	14	688	22	7.62	148	62	0.5<	15.8	1.04	5.79	2.9	118
H20	21.7	26.3	11	663	3	6.98	28	50<	0.5	13.2	0.77	5.25	4.5	326
H27	12.1	30.2	13	636	30	7.74	144	67	0.7	12	2.48	6.06	3.9	103
H31	25.5	33.2	20	728	25	8.79	151	82	0.5<	18	0.86	6.69	3	170
H35	26.5	31.2	16	697	21	8.14	143	59	0.5	18.8	0.93	6.17	2.3	177
H39	27.5	28.7	20	938	2	7.36	22	59	1.1	21.6	1.2	6.18	3.5	227
H43	14.7	18.6	9	649	37	4.84	125	61	0.5<	9.2	0.6	4.28	3.3	81.2
H46	14.9	31.8	12	644	30	8.12	143	50	1	12	5.88	6.45	4.3	110
H49	26.7	29.5	12	737	25	7.75	144	88	0.5<	15.7	1.03	5.87	2.5	140
H50	19.2	15.3	7	799	10	3.63	99	74	1.4	7.5	11.22	3.51	1.8	180
H55	18.6	31.6	14	765	28	8.36	154	102	0.5	18.3	1.54	6.33	2.9	127
H58	12.3	30.7	10	644	26	7.96	146	114	1.2	10.1	6.88	6.68	3.3	110
H64	22.5	29.4	11	718	25	7.75	160	87	0.6	14.6	0.63	5.88	2.7	171
H66	25.5	28	13	718	23	7.33	143	55	0.5<	14.8	0.91	5.66	3	133
H70	14.6	31.1	13	645	26	7.89	146	96	1	11.3	735	6.12	5.2	112
H71	11.6	28.6	10	543	27	7.39	128	50<	0.6	8.6	0.75	5.97	2.9	132
H73	14.8	36.6	18	642	27	9.46	94	50<	0.5	14.3	0.5<	7.08	2.5	148
H75	12.6	30.9	13	617	20	8.14	127	50<	0.5	10.7	0.5<	6.34	4.1	140
H76	28.9	29.1	14	725	23	7.8	123	61	0.5	15.5	1.52	5.87	2.3	178
H81	14	26	12	619	97	6.74	175	50<	1	10.8	1.07	5.12	4.6	87.2
H83	14.4	17.8	6	558	51	4.67	169	62	0.8	8	1.09	3.75	5.8	90.5
H84	16.8	21.8	8	599	59	5.81	167	53	0.9	9.1	0.95	4.71	5.8	99.9
H88	22.8	19.5	5	522	10	5.5	111	69	0.5<	9	0.5<	3.78	1.6	220
H91	11	22.7	4	416	12	6.55	133	55	0.5<	5.2	1.03	3.98	2.4	158
H95	32.4	35.7	10	921	18	8.52	127	93	0.5<	18.2	0.9	8.7	6.1	212
H96	18	28.9	9	716	17	7.2	125	69	0.5<	12.6	0.81	6.2	4	175
H97	9.7	18.4	5	414	10	5.09	103	53	0.5<	4.9	0.5<	3.33	3	166

Table 2 (cont.)

Sample	Ta	Tb	Te	Th	Ti	Tl	Tm	U	V	W	Y	Yb	Zn	Zr
Importar imagen	0.1	0.1	0.1	0.1	10	0.1	0.1	0.1	1	1	0.5	0.05	1	5
H1	0.75	0.71	0.1	12.07	4016	0.65	0.29	1.4	68	1.3	24.2	3	80	28
H2	1.03	0.74	0.26	16.72	2794	0.74	0.26	2.4	47	1.3	17	1.6	47	53
H13	1.23	0.47	0.23	9.14	4032	0.83	0.2	1.7	79	1<	12.9	1.3	99	13
H16	0.81	0.73	0.1 <	11.81	3571	0.63	0.33	1.1	58	1<	24.7	3.2	72	22
H20	0.73	0.76	0.1 <	11.08	3035	0.1 <	0.37	1.8	54	1<	28.9	3.5	10	12
H27	1	0.76	0.4	12.39	3396	0.65	0.26	1.2	59	1.3	19.3	1.8	62	12
H31	0.81	0.78	0.1 <	13.9	4161	0.71	0.25	1.1	66	1<	21	2.2	83	13
H35	0.8	0.74	0.1 <	13.01	4401	0.76	0.27	0.8	73	1.2	21.1	2.2	92	15
H39	0.82	0.93	0.1 <	15.62	5094	0.1 <	0.46	1.8	64	1<	37.4	5.1	81	24
H43	0.6	0.65	0.1 <	9.84	2082	0.64	0.24	1.1	40	1	21.7	1.7	56	36
H46	1.02	0.83	0.24	13.32	3267	0.68	0.33	1.2	52	1.4	22.8	2.5	67	10
H49	0.81	0.69	0.1 <	12.43	3796	0.64	0.2	0.8	58	1<	18.8	1.7	84	21
H50	1.37	0.51	0.48	11.59	3532	0.5	0.17	1.7	48	3.6	13.3	0.5	41	19
H55	0.64	0.73	0.1 <	13.29	4262	0.71	0.22	1	69	1<	19.3	2	103	17
H58	0.83	0.78	0.31	12.66	2923	0.69	0.36	1.8	47	1.2	23.9	2.8	61	12
H64	0.63	0.71	0.1 <	12.57	3544	0.73	0.23	1	56	1<	20.2	1.8	75	21
H66	0.68	0.71	0.1 <	11.88	3786	0.72	0.25	1.03	59	1<	21	2.3	77	24
H70	1.05	0.66	0.47	13.5	3345	0.7	0.19	0.88	53	1.2	15	0.9	72	8
H71	0.83	0.84	0.3	14.01	2499	0.6	0.31	1.1	43	1<	27.3	2.2	58	6
H73	0.9	0.8	0.14	14.77	4490	0.43	0.33	1	81	1<	23.2	3	75	6
H75	1	0.75	0.19	13.5	3256	0.61	0.28	0.9	57	1.1	22.2	2.2	62	11
H76	0.86	0.81	0.1 <	13.16	3813	0.51	0.28	1.4	69	1<	27.2	2.7	279	17
H81	0.96	0.69	0.15	12.25	3104	0.79	0.3	1.2	52	2.1	21.5	2.3	64	11
H83	0.61	0.5	0.1 <	8.48	1617	0.99	0.18	0.9	33	1.2	13.7	1.3	103	27
H84	0.68	0.64	0.1 <	9.57	1985	0.8	0.22	1.2	37	1<	18	1.5	117	29
H88	0.8	0.56	0.1 <	13.88	2934	0.57	0.31	2.7	62	1<	22	3.1	44	13
H91	1.01	0.57	0.27	16.83	2290	0.63	0.33	3.85	48	1<	20.9	2.8	26	6
H95	2.66	1.4	0.28	10.81	5439	0.62	0.97	3.1	130	1.3	57.2	12	84	29
H96	1.66	0.94	0.25	14.61	4126	0.61	0.57	3.5	86	2.2	35.9	6.1	74	17
H97	0.48	0.47	0.39	12.22	2221	0.52	0.26	1.6	47	1<	17.4	1.8	24	10

GEOLOGY OF THE REGION

With a 1000 km2 outcrop, the granitoid batholith of Shirkuh is located in the coordinates range 31° 23' to 31° 45' N and 53° 50' to 20° 54' E, in Yazd Province, southeast of Taft and west of Mehriz, Iran (Fig. 1).

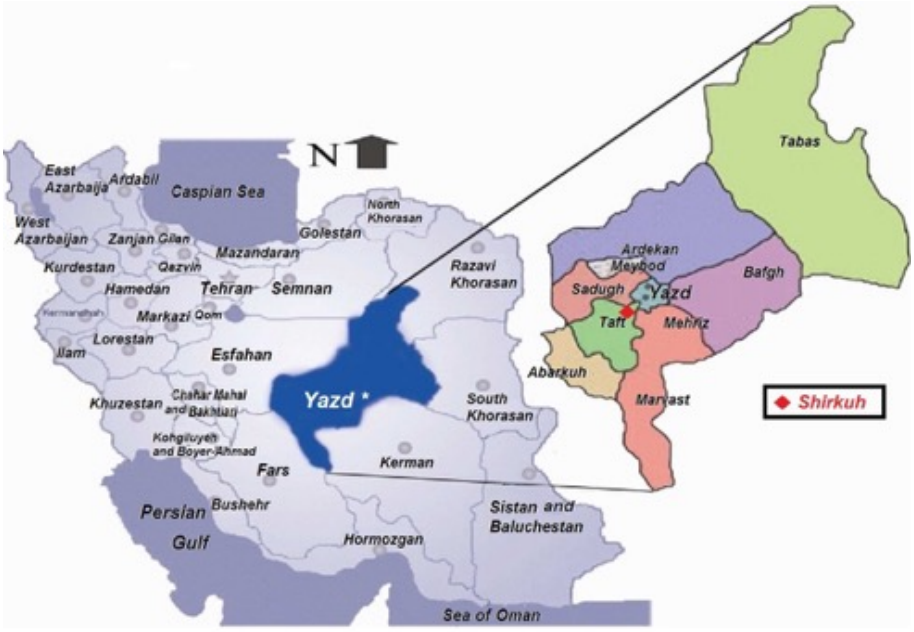

Figure 1 - Geography of Yazd Province on the map of Iran (courtesy of Natural Geography of Yazd Province).

According to the structural zones of Iran, the study range is situated in Central Iran (STOCKLIN, 1988) and in the middle of the Urmia–Dokhtar volcanic belt (Fig. 2). The geological map of Iran (courtesy of MOINE-VAZIRI, 1985) dates back this region to the volcanic period of The Paleocene. Shirkuh batholith, having cut through the Nayband formation (Upper Triassic) with Cretaceous limestones and a sandstone and conglomerate unit (Lower Cretaceous) lying on top as an angular unconformity, probably dates back to the Jurassic.

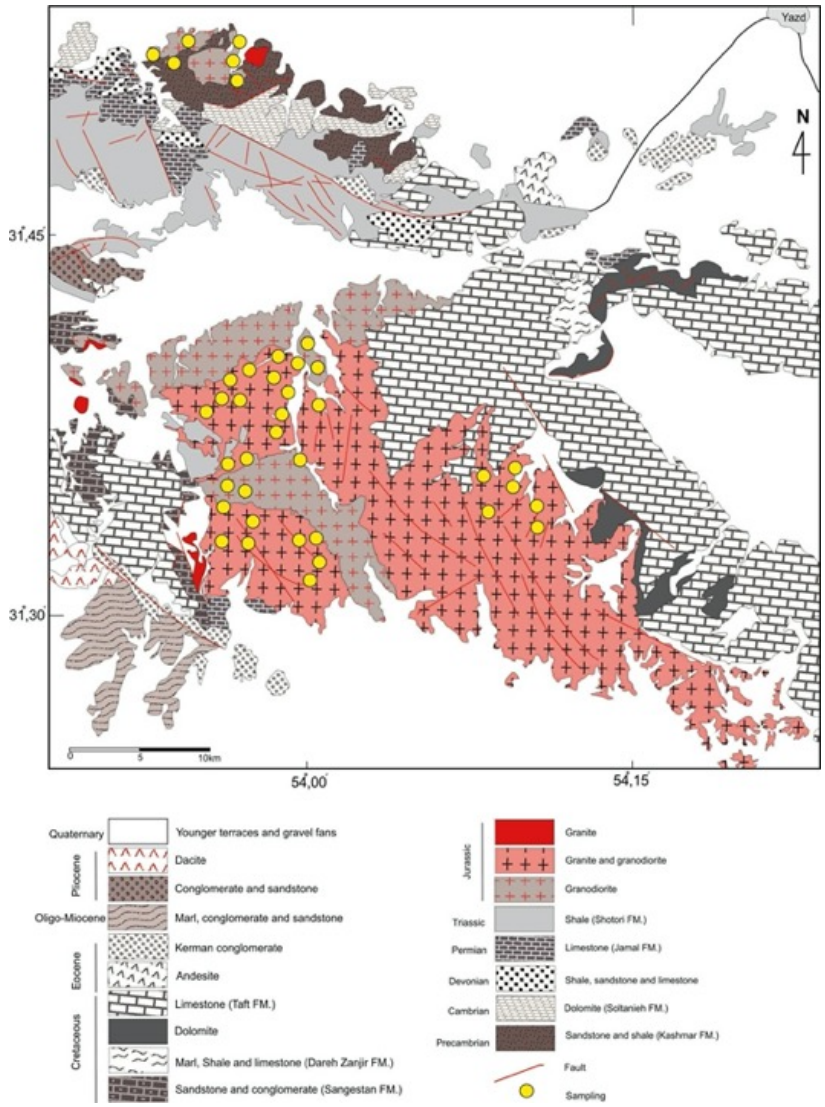

Figure 2 - The situation of the study region east of the 1:100000 map of Khezrabad (HAJMOLLA'ALI, 1993), west of the 1:100000 map of Yazd (HAJMOLLA'ALI, 2000), north of the 1:100000 map of Nir (SHAHRAKI GHADIMI, 2008), and north of the 1:100000 map of Dehshir (SABZE'I, 1997).

The Shirkuh granite is younger than the Nayband formation but older than those from the Cretaceous. Forster (1972) dated the Shirkuh granite by the Rb–Sr method at 176±10 million years, whereas Rir and Mohafez (1972) dated the Shirkuh granitoid feldspars at 159–186 million years by the K–Ar method.

The said batholith is composed of five rock units, namely monzogranite, granodiorite, quartz monzonite, quartz monzodiorite, and syenogranite. Monzogranites, as the largest unit, form the main body of the batholith.

CHEMISTRY OF MINERALS

The mineral sets are classified into five rock units, including plagioclase, quartz, and orthos—as the main minerals—and biotite, muscovite, garnet, tourmaline, amphibole, epidote, zircon, sphene, and apatite—as accessory minerals. An accurate petrographic study reveals each mineral to account for a different share.

This study addresses the mineralogical details and petrological concepts of the minerals.

Plagioclase

The table below (Table 3) presents the analysis results for the plagioclases.

Table 3 - The EMP analysis results for the plagioclase in different Shirkuh granitoid batholith units.

Quartzmonzodiorite										
	Importar imagen	Importar imagen	Importar imagen	Importar imagen	Importar imagen	Importar imagen	Importar imagen	Importar imagen	Importar imagen	Importar imagen
100-1	61.58	0.1	20.64	0.52	-	10.97	5.35	0.7	-	50.9
100-2	60.8	0.14	21.45	0.42	-	11.11	5.43	0.58	-	51.4
100-4	61.75	-	21.02	0.43	-	10.17	5.82	0.75	-	47.1
100-5	59.88	-	21.72	0.37	-	12.05	5.35	0.56	-	53.8
100-8	60.8	-	20.29	0.43	-	9.98	7.9	0.47	0.08	40.2
100-9	59.8	-	22.93	0.89	-	14.6	0.01	0.82	0.89	93.6
100-10	62.14	-	20.96	0.52	-	9.68	6.19	0.45	0.02	45.2
100-11	63.46	-	21.11	0.58	-	11.25	3.08	0.44	0.04	64.8
100-14	61.55	-	22.24	1.11	-	12.19	1.54	0.9	0.47	76
100-18	59.05	-	22.11	0.49	-	11.83	5.32	1.08	-	52
100-19	59.15	-	21.86	0.38	-	9.68	8.39	0.49	-	38

Table 3 (cont.)

Quartzmonzodiorite										
	Importar imagen	Importar imagen	Importar imagen	Importar imagen	Importar imagen	Importar imagen	Importar imagen	Importar imagen	Importar imagen	Importar imagen
13-6	57.29	0.78	22.43	0.21	-	11.27	6.35	1.61	-	45.7
13-7	58.45	0.85	20.25	0.25	-	12.11	5.75	2.25	-	48.1
13-8	58.64	-	22.37	0.41	-	12.65	4.75	1.14	-	55.9
13-9	57.68	-	21.84	0.39	-	13.54	6	0.49	-	54.2
13-10	62.15	-	19.37	0.37	-	13.04	4.62	0.39	-	59.6
13-12	56.41	-	18.96	1.35	-	11.8	0.53	10.88	-	45.9
13-13	55.63	-	23.53	0.76	-	17.46	1.52	1.04	-	81.4
13-14	60.1	-	21.79	0.53	-	12.9	3.9	0.72	-	62
13-19	60.42	-	20.38	0.56	-	13.02	4.57	1	-	57.9
13-20	57.96	-	22.61	0.48	-	15.04	3.12	0.74	-	69.7
13-21	87.54	-	6.17	0.17	-	3.88	1.76	0.45	-	51

Table 3 (cont.)

Syenogranite

	Importar imagen	Importar imagen	Importar imagen	Importar imagen	Importar imagen	Importar imagen	Importar imagen	Importar imagen	Importar imagen	Importar imagen
98-1	60.64	-	20.4	0.5	-	11.06	6.45	0.71	0.17	46.9
98-2	63.15	-	19.66	0.5	-	11.58	3.91	1.07	0.06	58.1
98-3	61.87	0.08	20.92	0.48	-	11.87	3.56	0.84	-	61.5
98-4	63.12	0.08	19.96	0.39	-	10.68	4.93	0.52	-	52.8
98-5	96.75	0.57	0.73	0.08	-	0.18	1.43	0.21	-	5.8
98-6	73.83	-	15.62	0.29	-	4.53	5.14	0.49	0.1	31.4
98-7	73.65	-	13.55	0.29	-	4.16	7.81	0.47	0.06	22.1
98-8	64.73	-	18.35	0.34	-	6.44	8.92	1.09	0.08	27
98-9	79.61	-	8.03	0.06	-	1.22	3.97	7.01	0.05	7.3
98-10	69.32	-	18.48	0.24	-	6.34	4.52	1.08	-	40
98-11	71.49	-	16.79	0.21	-	4.28	5.28	1.92	-	26.5
98-12	68.11	-	16.45	0.34	-	6.71	7.14	0.98	-	32.3
98-13	66.27	-	17.84	0.3	-	5.92	8.17	0.82	-	26.1

Table 3 (cont.)

Granodiorite

	Importar imagen	Importar imagen	Importar imagen	Importar imagen	Importar imagen	Importar imagen	Importar imagen	Importar imagen	Importar imagen	Importar imagen
69-1	62.26	-	21.59	0.24	-	9.86	4.07	1.91	-	50.6
69-2	62.3	-	20.33	0.15	-	7.2	8.63	1.34	-	29.5
69-3	64.1	-	18.14	0.16	0.09	6.29	10.04	0.71	-	24.9
69-4	64.83	-	18.91	0.14	0.08	6.84	8.13	0.62	-	30.7
69-5	65.51	-	20.02	0.2	0.01	7.35	5.25	1.21	-	39.1
69-6	63.19	-	21.6	0.26	0.01	8.17	4.39	2.29	-	43.4
69-7	68.51	-	18.56	0.09	-	3.76	8.37	0.65	-	19.1
69-8	63.96	-	22.35	0.21	-	6.74	3.95	2.74	-	39.3
69-9	66.8	-	18.52	0.23	-	5.35	7.42	0.83	-	27
69-10	66.76	-	19.28	0.17	-	6.01	6.97	0.13	-	30.9

Table 3 (cont.)

Quartsmonzonite

	Importar imagen	Importar imagen	Importar imagen	Importar imagen	Importar imagen	Importar imagen	Importar imagen	Importar imagen	Importar imagen	Importar imagen
37-1	59.52	-	22.98	0.47	-	11	3.77	2.19	-	53.8
37-2	58.06	-	23.84	0.87	-	11.9	4.1	1.88	-	53.7
37-3	60.24	-	22.58	0.35	-	9.98	3.29	3.51	-	49.6
37-4	60.59	-	22.36	0.25	-	11.89	3.6	1.26	-	59.7
37-5	61.57	-	21.18	0.36	-	9.13	4.46	3.25	-	43.3
37-6	59.03	-	22.05	0.24	-	13.16	4.76	0.7	-	58.2
37-7	59.03	-	22.05	0.24	-	13.16	4.76	0.7	-	58.2

Table 3 (cont.)

Monzogranite										
	Importar imagen	Importar imagen	Importar imagen	Importar imagen	Importar imagen	Importar imagen	Importar imagen	Importar imagen	Importar imagen	Importar imagen
88-1	62.46	-	20.33	0.52	-	11.36	4.47	0.79	-	55.7
88-2	60.27	-	20.13	0.37	-	9.5	8.74	0.94	-	35.9
88-3	64.02	-	20.89	0.44	-	11.13	2.34	1.11	-	66.7
88-10	61.17	-	20.79	0.39	-	9.8	7.36	0.5	-	41.3
88-11	62.58	-	20.33	0.45	-	10.43	5.26	0.73	-	50.1

Table 3 (cont.)

Monzogranite										
	Importar imagen	Importar imagen	Importar imagen	Importar imagen	Importar imagen	Importar imagen	Importar imagen	Importar imagen	Importar imagen	Importar imagen
44-1	56.97	-	23.19	0.19	0.04	12.73	6.23	0.59	-	51.5
44-2	58.18	-	22.1	0.24	0.03	14.35	4.39	0.64	-	62.2
44-3	61.23	-	21.77	0.19	0.03	12.56	3.59	0.48	-	64.1
44-4	89.21	-	6.39	0.11	0.15	2.66	1.26	0.18	-	51.6
44-5	59.07	-	21.35	0.11	-	11.73	7.21	0.49	-	46.2
44-6	59.01	-	22.58	0.11	-	14.14	3.66	0.43	-	66.5
44-7	59.5	-	21.85	0.14	-	12.35	5.53	0.57	-	53.6
44-8	60.94	-	21.47	0.18	-	13.01	3.61	0.75	-	63.7
44-9	60.92	-	22.88	0.19	-	13.06	2.33	0.57	-	72.7
44-10	60.03	-	23.52	0.2	-	12.41	3.25	0.54	-	65.5
44-11	59.21	-	21.09	0.21	-	12.1	6.83	0.51	-	48.3
44-12	55.75	-	22.09	0.2	0.07	12.77	8.26	0.8	-	44.5
44-13	58.64	-	22.74	0.19	0.16	12.73	4.51	0.98	-	57.7
44-14	58.77	-	21.36	0.25	0.13	10.48	6.04	2.92	-	42.1
44-15	60.25	-	22.37	0.18	0.19	10.64	4.44	1.88	-	50.9

Table 3 (cont.)

Monzogranite										
	Importar imagen	Importar imagen	Importar imagen	Importar imagen	Importar imagen	Importar imagen	Importar imagen	Importar imagen	Importar imagen	Importar imagen
46-1	56.83	-	22.57	0.19	-	13.53	6	0.81	-	53.4
46-2	60.48	-	21.76	0.13	-	13	4.04	0.52	-	62.1
46-3	58.34	-	21.36	0.15	-	13.44	6.2	0.42	-	53.4
46-4	59.1	-	22.96	0.15	-	13.53	2.94	0.69	-	68.8
46-5	56.32	-	20.28	0.14	-	12.79	9.29	0.52	-	42.3
46-6	57.69	-	22.44	0.16	-	13.48	5.38	0.5	-	56.6
46-7	58.58	-	21.47	0.08	-	12.41	7.18	0.27	-	48.2
46-8	59.23	-	21.76	0.16	-	13.04	5.31	0.44	-	56.3
46-9	57.62	-	21.75	0.13	-	13.6	6.59	0.32	-	52.5
46-10	56.32	-	22.13	0.26	-	12.05	8.97	0.23	-	42.2
46-11	56.66	-	23.18	0.19	-	13.31	6.38	0.24	-	52.9
46-12	61.59	-	22.76	0.26	-	15	-	0.34	-	97.4
46-14	59.04	0.56	22.3	0.12	0.03	12.09	5.31	0.5	-	54.2
46-15	58.86	0.52	21.32	0.1	0.03	11.24	7.6	0.3	-	44.3
46-16	58.87	0.62	20.22	0.12	0.03	11.57	7.028	0.54	-	45.6

Table 3 (cont.)

Monzogranite

	Importar imagen	Importar imagen	Importar imagen	Importar imagen	Importar imagen	Importar imagen	Importar imagen	Importar imagen	Importar imagen	Importar imagen
82-1	60.22	-	22.9	0.21	-	14.13	1.82	0.65	-	77.6
82-2	59.53	-	21.63	0.19	-	12.76	5.2	0.63	-	55.7
82-5	59.28	-	21.21	0.39	-	14.43	3.16	1.46	-	65.9
82-6	58.71	-	21.71	0.16	-	12.85	6.09	0.42	-	52.7
82-7	87.85	-	4.72	0.23	-	1	1.21	4.95	-	11
82-8	69.35	-	12.06	0.07	-	0.38	2.07	16.01	-	1.6
82-9	61.52	-	21.06	0.21	-	10.97	4.07	2.12	-	52.6
82-10	57.01	-	21.79	0.16	-	14.82	5.7	0.47	-	57.7
82-11	56.93	-	23.35	0.15	-	12.99	6.16	0.42	-	52.7
82-12	60.39	-	22.24	0.18	-	13.39	3.3	0.51	-	67.1
82-13	59.98	-	22.67	0.07	-	12.83	3.89	0.56	-	62.5

Table 3 (cont.)

Monzogranite

	Importar imagen	Importar imagen	Importar imagen	Importar imagen	Importar imagen	Importar imagen	Importar imagen	Importar imagen	Importar imagen	Importar imagen
81-1	72.22	-	18.47	0.06	0.01	3.71	4.79	0.72	-	28
81-2	72.22	-	18.47	0.06	0.01	3.71	4.79	0.72	-	28
81-3	67.37	-	18.15	0.05	-	4.18	9.33	0.92	-	18.9
81-4	66.96	-	18.79	0.03	-	4.88	8.49	0.85	-	22.9

Table 3 (cont.)

Quartzmonzonite

	Importar imagen	Importar imagen	Importar imagen	Importar imagen	Importar imagen	Importar imagen	Importar imagen	Importar imagen	Importar imagen	Importar imagen
95-1	60.35	-	21.46	0.54	-	11.97	3.91	1.24	-	58.3
95-2	49.85	-	25.06	0.97	-	18.76	4.37	0.43	-	69
95-5	61.82	-	21.4	0.7	0.12	10.36	4.51	1.04	-	52.4
95-6	63.8	-	19.62	0.45	0.11	10.05	4.12	1.8	-	51.1
95-9	61.77	-	19.74	0.72	-	9.58	6.97	1.21	0.01	40.5
95-10	60.76	-	20.34	0.43	-	11.62	6.16	0.54	0.15	49.6
95-13	63.56	-	22.31	0.73	-	10.37	1.9	0.98	0.1	69.3
95-14	64.1	-	21.62	0.47	-	11.2	1.47	1.05	0.04	74.1

Table 3 (cont.)

Quartzmonzonite										
	Importar imagen	Importar imagen	Importar imagen	Importar imagen	Importar imagen	Importar imagen	Importar imagen	Importar imagen	Importar imagen	Importar imagen
35-6	59.74	-	20.69	0.13	-	12.38	6.17	0.83	-	50.5
35-7	59.34	-	21.33	0.18	-	12.52	5.49	1.09	-	52.7
35-8	59.09	-	21.86	0.13	-	11.49	6.32	1.07	-	47.5
35-9	59.34	-	21.33	0.18	-	12.52	5.49	1.09	-	52.7
35-10	59.34	-	21.33	0.18	-	12.52	5.49	1.09	-	52.7
35-11	59.02	-	22.07	0.14	0.26	13.95	3.94	0.56	-	64.1
35-12	56.89	-	23.01	1.2	0.23	12.1	6.19	0.3	-	51.1
35-13	59.53	-	22.03	0.19	0.19	13.2	4.19	0.62	-	61.3

The anorthite content is calculated and presented based on the analysis results and the weight percent and atomic percent of the elements for each point on the analyzed cross-section. The zoning is based on the anorthite content at the plagioclase core and rim, as well as its variations, which at last helps identify the plagioclase.

In the monzogranite unit, some plagioclases feature reverse zoning and others oscillatory zoning. Further, plagioclases outcrop with reverse and regular zoning in syenogranites and granodiorites. Plagioclases of the quartz monzodiorite unit exhibit both oscillatory and reverse zoning, while those of the quartz monzonite show no zoning (YAZDI et al., 2017 and 2019) (Fig. 3).

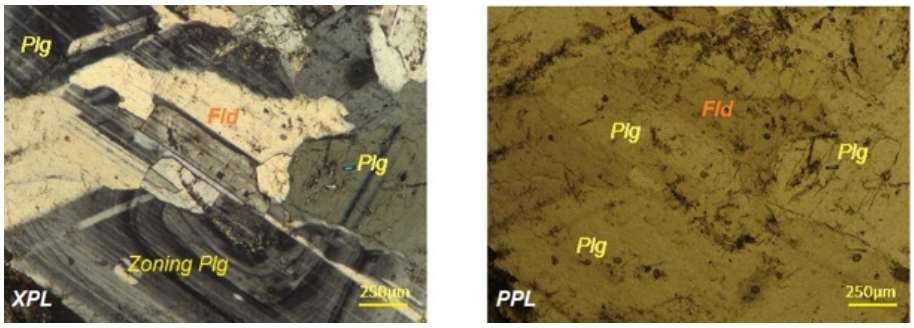

Figure 3 - Regular and oscillatory zoning in the plagioclase.

Amphibole

The table below (Table 4) presents the analysis results for the amphibole.

Table 4 - The EMP analysis results for the amphibole in different Shirkuh granitoid batholith units.

	Importar imagen	Importar imagen	Importar imagen	Importar imagen	Importar imagen	Importar imagen	Importar imagen	Importar imagen	Importar imagen
100-3	39.44	3.48	4.66	21.54	0.64	10.8	13.52	0.83	-
100-6	41.75	2.42	4.69	23.03	0.83	8.57	13.55	0.98	-
100-7	40.86	2.02	4.75	23.81	0.65	9.65	13.77	0.86	-
100-12	38.82	3.02	4.48	21.52	0.78	10.63	13.88	0.84	0.83
100-13	42.1	1.34	3.52	22.43	0.99	10.01	14.69	0.55	1.01
100-16	37.21	12.99	3.34	4.35	0.63	7.58	18.56	0.36	-
100-17	42.32	3.34	4.95	20.25	0.66	8.96	13.36	1.02	-
95-3	38.58	2.49	6.17	23.79	0.99	9.27	13.4	0.85	-
95-4	40.84	1.33	3.88	25.25	1.44	10.71	12.72	0.62	-
95-7	37.34	3.21	5.71	26.98	1.37	8.38	9.47	2.75	-
95-8	40.51	2.17	4.28	25.72	1.27	9.37	11.08	1.84	-
95-11	41.45	2.51	5.4	22.04	0.75	9.09	12.82	1.36	-
95-12	41.39	2.13	5.43	23.04	0.9	9.36	12.69	0.79	-
95-15	40.72	2.43	5.71	21.16	0.88	9.68	13.85	1.16	0.17
95-16	41.24	2.17	5.03	20.01	0.82	9.67	14.77	1.04	1.18
88-4	40.4	2.14	4.91	22.8	0.77	10.31	14.04	0.8	-
88-5	43.66	1.91	6.52	20.71	0.84	8.52	13.48	0.69	-
88-6	41.77	1.77	4.33	23.79	1.14	10.4	13.12	0.5	-
88-7	41.88	1.44	3.99	25.04	1.36	9.32	13.39	0.51	-
88-8	39.46	1.74	4.36	25.53	1.15	9.18	13.86	0.82	0.5
88-9	39.46	1.74	4.36	25.53	1.15	9.18	13.86	0.82	0.5
88-12	37.84	2.21	4.31	21.98	0.75	10.06	15.62	0.78	2.63
88-13	38.86	1.95	5.03	22.94	0.74	10.82	14.09	0.79	1.11
88-14	38.55	1.75	5.39	28.16	1.02	9.94	11.29	0.51	0.01
88-15	41.33	1.91	4.39	24.01	1	9.89	13.19	0.61	0.06
88-16	40.14	1.98	4.35	24.66	1.05	9.72	13.68	0.71	-
88-17	40.65	1.67	4.49	25.25	1.22	8.94	13.6	0.68	-
13-5	42.73	0.91	4.51	26.27	0.97	7.33	13.88	0.88	-
13-22	46.14	0.72	3.95	25.62	1.03	8.04	11.38	0.78	-
13-23	41.25	1.48	5.14	26.2	1.06	6.84	13.06	1.89	-

Amphiboles are abundant in both igneous and metasomatic rocks alike. They may occur in any igneous rock from acidic to basic. However, the intermediates are considerably more common in plutonic igneous rocks (DANA, 1985). In some samples, amphibole is the main mineral, while in others, it is an accessory one. Amphiboles are prevalent in automorphic and subautomorphic forms in the samples, except for quartz monzodiorite and monzogranite (Fig. 4).

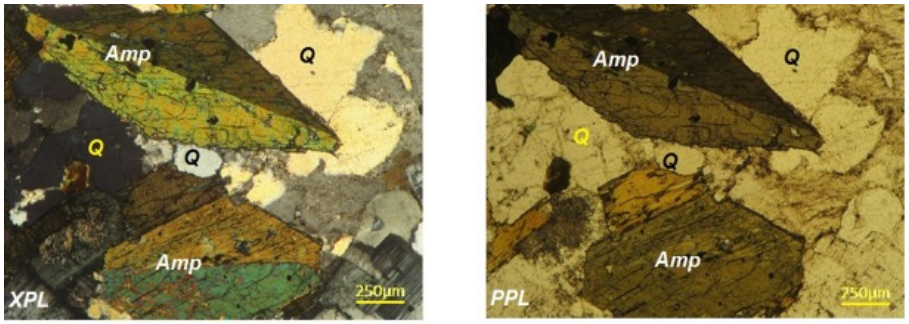

Figure 4 - Automorphic amphibole in quartz monzodiorite

The EMP analysis of amphiboles based on the structural formula of amphibole and for an average 13–15 cations (Avg15-NK,13-CNK) indicated that the amphiboles are of the tschermakite, ferro-hornblende, and tschermakite hornblende varieties. Given that Importar imagen is greater than 1 in the structural formula of the current amphiboles in the quartz monzodiorite and monzogranite of the region, the prefix "ferro" can be used to name the hornblendes. Based on the classification of Leak et al. (1997), although the amphiboles of the Shirkuh batholith can be classified into Mn, Mg, Fe and calcic groups, they are mainly of the latter type (Fig. 5).

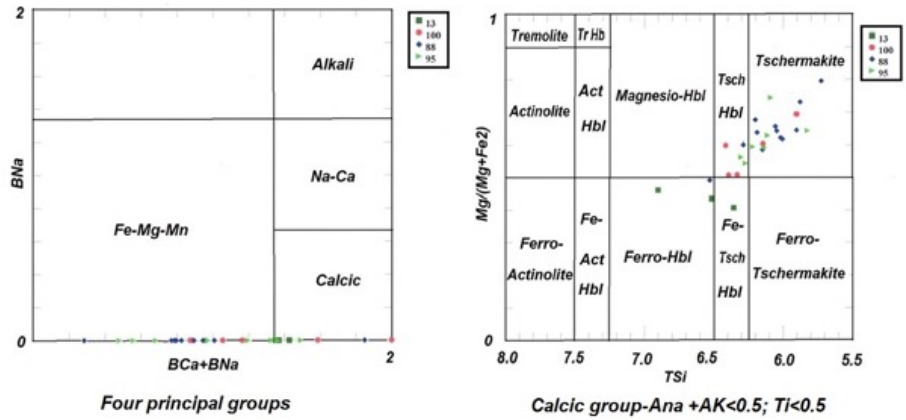

Figure 5 - Classification of amphiboles based on 13 and 15 cations on average (Avg15-NK, 13-CNK).

According to the Si versus Na+Ca+K plot presented by Leake (1971), all analyzed points of the studied amphibole fall in the magmatic (igneous) amphibole category (Fig. 6).

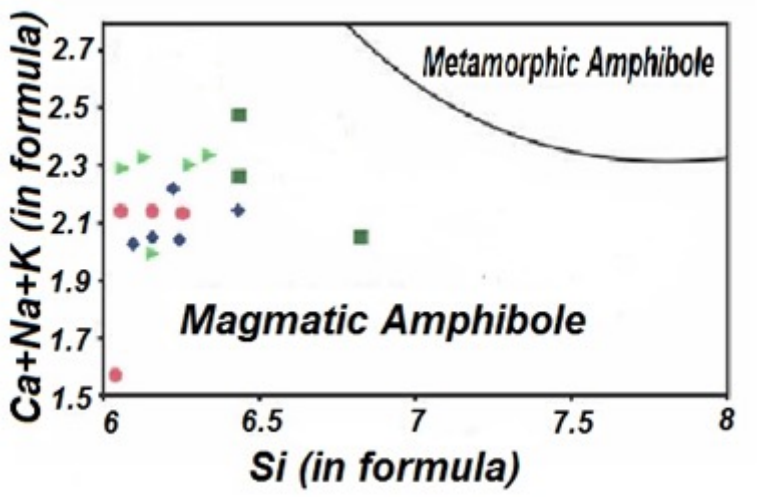

Figure 6 - The composition of amphibole crystals in the Shirkuh intrusive rock mass, all points of which fall into the igneous amphibole category Leake (1971).

Biotite

In general, biotite is the only mafic mineral in the composition of the Shirkuh generic batholith. The mineral appears in monzogranites in an intact form but is bent at times. Further, it is chloritized in some samples. In quartz monzodiorite and granodiorite, biotite is severely chloritized and opacitized and has a high content of opaque and apatite inclusions. Biotites are bent at times, which is indicative of their exposure to pressure (Fig. 7). In syenogranites, biotite is present as an accessory mineral (NOVRUZOV et al., 2019).

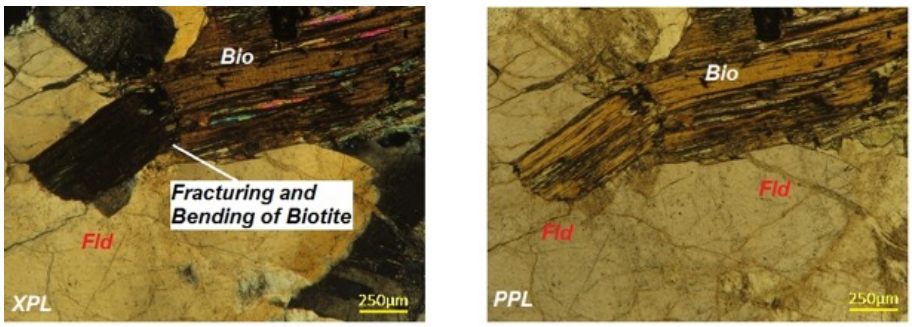

Figure 7 - Signs of bending and fracture are apparent in biotites due to tectonic pressure.

ACCESSORY MINERALS OF THE SHIRKUH GRANITOID BATHOLITH

Garnet

The table below (Table 5) presents the analysis results for the garnet.

Table 5 - The EMP analysis results for the garnet in different Shirkuh granitoid batholith units.

	Importar imagen	Importar imagen	Importar imagen	Importar imagen	Importar imagen	Importar imagen	Importar imagen	Importar imagen	Importar imagen	Importar imagen
82-3	27.81	-	15.29	48.05	3.67	3.75	1.32	-	-	-
82-4	29.86	-	12.4	49.81	3.67	2.88	1.28	-	-	-
82-2-1	26.13	-	12.06	52.9	4.23	3.11	1.37	-	-	-
82-2-2	28.16	-	13.46	47.11	4.79	2.99	1.38	-	-	-
81-2-1	34.92	-	14.56	36.42	4.81	-	2.3	4.44	1.64	-
81-2-2	32.11	-	14.62	44.8	3.62	2.19	1.37	-	1.19	-
81-2-3	29.97	-	13.15	48.2	3.72	3.02	1.37	-	0.47	-
81-2-4	28.6	-	13.02	51.09	4.09	1.76	1.27	-	0.07	-
46-17	64.22	-	14.63	0.12	-	-	0.68	2.23	18.11	-
35-1	61.56	0.44	-	1.35	-	-	28.53	-	1.57	5.21
35-2	67.67	0.41	-	0.92	-	3.15	22.39	-	1.14	2.74
35-3	59.89	0.49	2.85	1.05	-	-	27.34	0.02	1.2	3.89
35-4	63.72	0.36	0.35	1.29	-	-	17.57	0.01	1.33	5.11
35-5	62.47	0.4	0.76	1.04	-	-	27.7	2.99	1.38	3.03

In microscopic observations, the garnet was found in semi-crystalline to amorphous form with irregular fractures in a quartz matrix and a dominant relationship with biotite (Fig. 8). Quartz inclusions can also be found in these garnets. However, no inclusion of metasomatic minerals was identified, which can be due to the igneous nature of garnet crystals (ANDERSON,1984). The texture gives no evidence attributing the formation of garnets to the biotite-consuming reactions (ALLAN and CLARCE,1981).

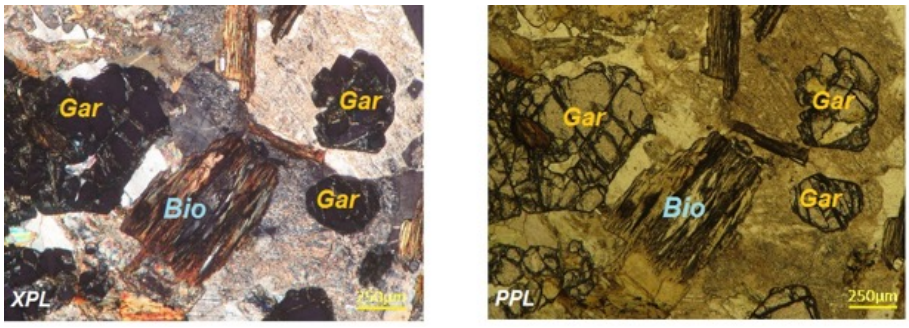

Figure 8 - Semi-crystalline to amorphous garnets.

Further, no trace of reaction rim or symplectic replacement was detected in microscopic investigations, which indicates the igneous origin of the garnet (Kawabata and Takafuji, 2005). A microscopic investigation of garnet crystals showed them to be void of chemical zoning. Further, the similarity of the inclusions in garnets with mineral phases of the host rock can be raised as another proof of their igneous origin (HARANGI et al., 2001).

The chemical analysis results for granitoid garnets from this region can be classified into pyralspite (pyrope, almandine, spessartine) and ugrandite (uvarovite, grossular, and andradite).

Based on the EMP results, the garnets collected from Lay Dal village have high chromium and calcium contents and, hence, are uvarovite and grossular. Moreover, garnets of the Saeidabad region can be said to have a limited composition spectrum as they are rich in iron and are of the almandine type (Fig. 9) but have low magnesium, calcium, and manganese contents. Garnets of a xenocrystic origin feature a wide composition variation range, while composition changes are limited in primary garnets (GREEN,1977; KAWABATA and TAKAFUJI, 2005). On the other hand, garnet-containing samples from Lay Dal (west of the rock mass) have high chromium and calcium contents. Another sample was found to be rich in potassium, which is an evidence for the igneous origin of the garnets crystallizing directly from the granitic melt. Moreover, the lack of distinctive zoning in the garnet can show that the mineral is not of metasomatic origin (Fig. 10).

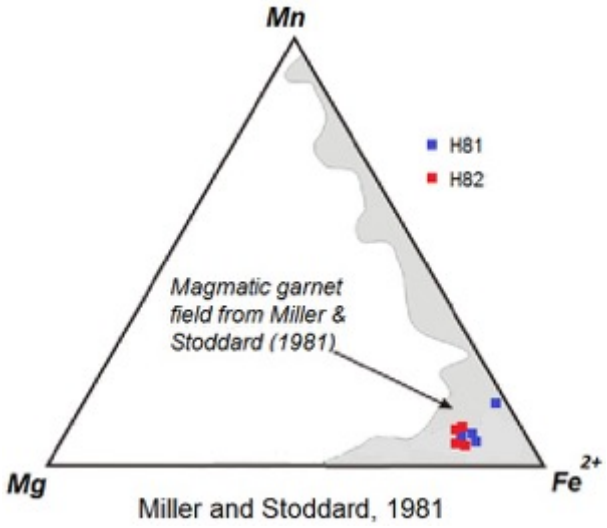

Figure 9 - EMP analysis results for the iron-rich Saeidabad region.

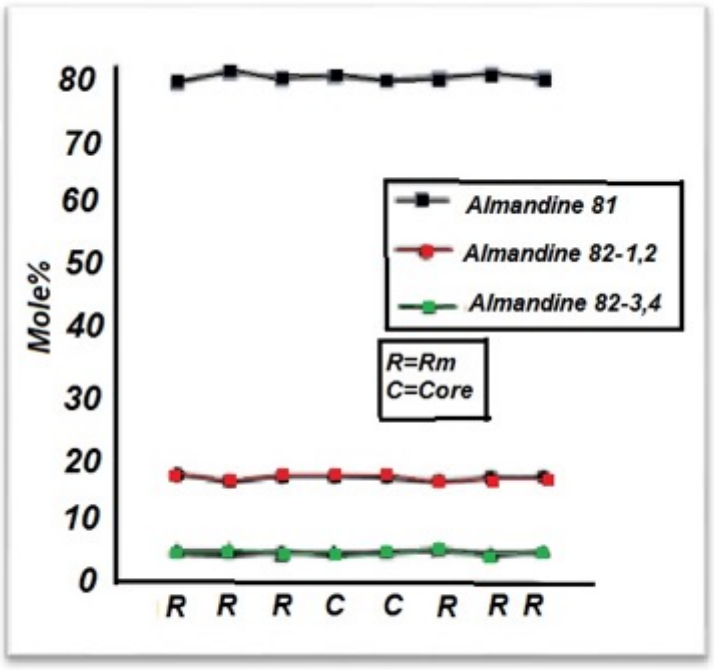

Figure 10 - The lack of zoning in local garnets (Gharib, 2012).

Tourmaline

Tourmaline in igneous rocks (Figure 11) can be categorized into magmatic and hydrothermal types with distinct microscopic properties (LONDON and MANNING, 1995). Automorphic and zone-free magmatic tourmalines crystallize under specific conditions—for example peraluminic and acidic conditions —showing that the primary magma was rich in boron (PESQUERA et al., 1999).

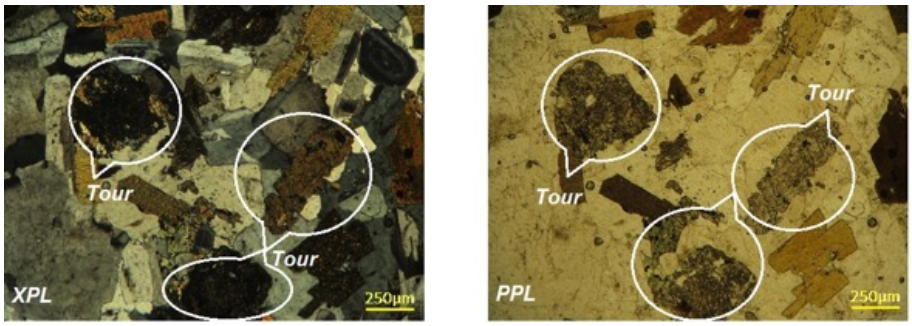

Figure 11 – Tourmalines.

Further, magmatic tourmalines have a higher Al content in comparison with their hydrothermal counterparts and feature a greater reduction at the X site (TRUMBULL and CHAUSSIDON, 1999). Moreover, Fe is present in a higher content than Mg (Cavarretta & Puxeddu, 1990). Hydrothermal tourmalines form by the reaction of boron-rich hydrothermal solutions with the wall rock (PILMER, 1988; KHODAMI and KAMALI SHERVEDANI, 2018). The tourmalines feature chemical zoning and have a higher Mg content than Fe. The zoning in tourmalines is indicative of sudden changes in temperature, pressure, fluid composition, or rapid non-equilibrium crystallization in an open chemical system (LONDON and MANNING, 1995).

Table 6 - The EMP analysis results are presented in the table below for nine points of the studied tourmalines.

	Importar imagen	Importar imagen	Importar imagen	Importar imagen	Importar imagen	Importar imagen	Importar imagen	Importar imagen	Importar imagen	Importar imagen
13-1	40.84	0.27	1.82	37.83	1.31	15.63	1.89	0.05	0.2	0.15
13-2	39.13	0.19	1.21	40.22	1.6	11.09	3.67	0.19	2.6	0.1
13-3	40.47	0.35	1.91	41.58	1.96	10.21	2.35	0.63	0.41	0.11
13-4	39.9	1.56	0.95	40.97	1.98	10.92	2.76	0.03	0.82	0.1
13-11	47.58	-	0.76	35.19	1.99	10.86	2.88	0.23	0.51	-
13-15	47.38	-	2.09	36.46	2.25	9.24	2.35	-	-	0.11
13-16	47.25	-	1.2	34.87	2.43	11.15	2.89	-	-	0.11
13-17	49.59	0.13	1.52	31.49	2.03	9.05	4.55	0.24	1.32	0.08
13-18	43	0.11	2.39	32.99	1.85	9.78	6.02	0.27	3.5	0.1

Based on the ternary X-Site-vacancy–(1-Ca+Na+K)-Na+(K)–Ca plot, tourmalines can be classified into calcic, alkali, and X-site-vacant types (HAWTHORNE and HENRY, 1999) (Fig. 12).

According to this classification, the composition of the tourmalines in the local quartz monzodiorite falls in the calcic range and the X-site-vacant type, which is indicative of the low Na+K content in comparison with Ca at the X site.

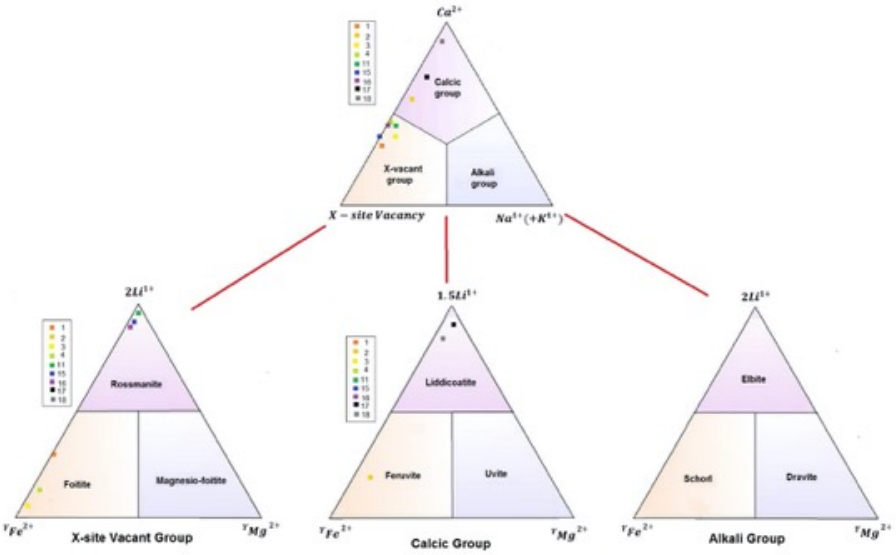

Figure 12 - Classification of tourmalines (HAWTHORNE and HENRY, 1999).

Further, Yavuz (2014) classified tourmalines as follows (Fig. 13).

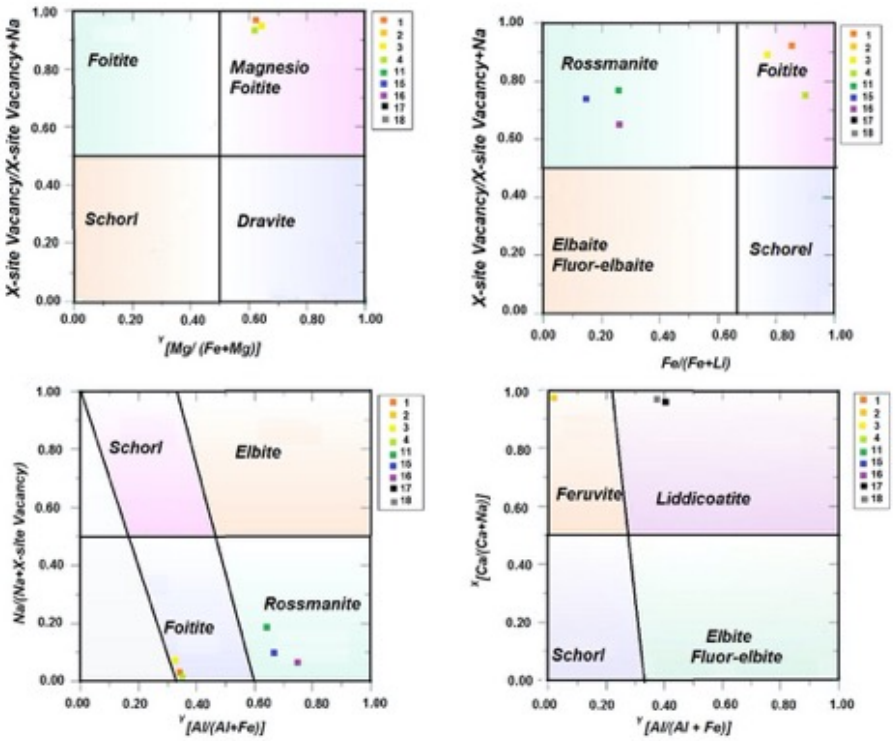

Figure 13 - The naming of tourmalines based on Yavuz's (2014) classification.

Samples 1, 3, and 4 have a high Mg content and, therefore, belong to magnesium-rich foitites.

Sample 2 belongs to the feruvite group.

Samples 5, 6, and 7 are rossmanites.

Samples 8 and 9 fall in the liddicoatite range.

According to Pirjaneou and Smiths (1992) who studied FeO/FeO+MgO (Fe#) variations against MgO in tourmalines, the Fe# level drops in the tourmaline away from the granite rock mass (Figure 14).

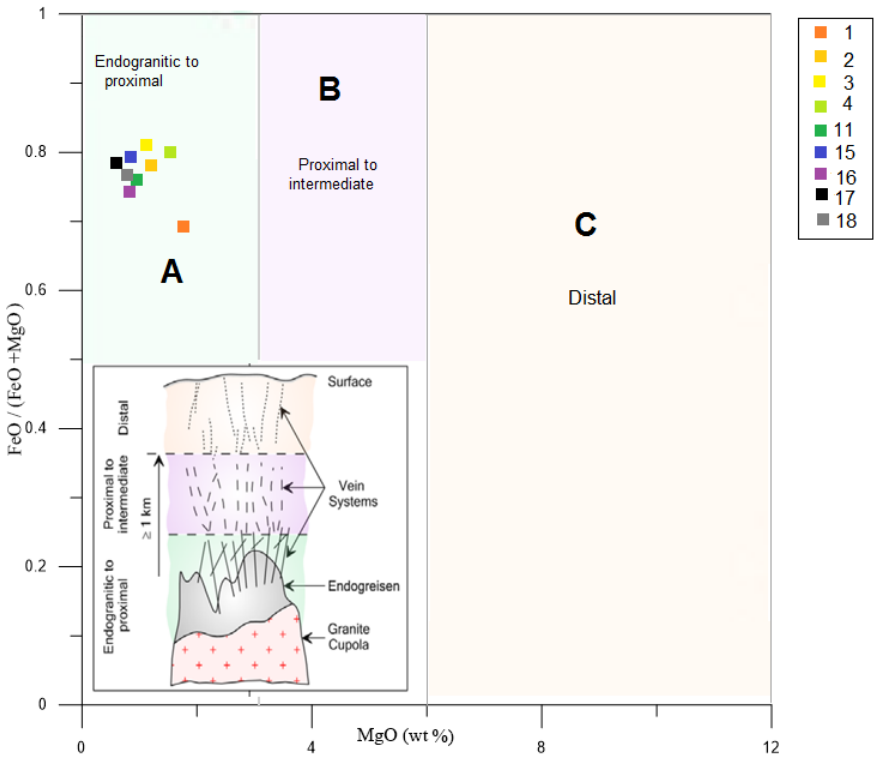

Figure 14 - The naming of tourmalines based on Pirjaneou and Smiths (1992) classification

A: The closed magmatic system, the positioning of the tourmalines inside and near the granite mass, and the lack of interference of external fluids in the formation of tourmalines.

B: Indicator of tourmalines located near or in the middle of the granite mass, and suggestive of the role of both magmatic and hydrothermal fluids in their formation.

C: Indicator of tourmalines farther from the granite mass and evidence determining the external source of boron and the hydrothermal nature of the system.

According to the figure, the tourmaline samples belong to the A region.

Zircon

Zircon is often the most important accessory mineral in granite rocks. Given its formation during the early stages of crystallization, Zircon mostly appears as inclusion in biotites, but is also found in its free form. Some igneous rocks feature circular zircon crystals that can probably be attributed to the absorption at the rim of mineral crystals by the primary melt (JOHAN and JOHAN, 2005). A pleochroic halo—resulting from the radioactive effects of some specific elements in the mineral—often surrounds zircon grains (MOBASHERGARMI et al., 2018) (Fig. 15).

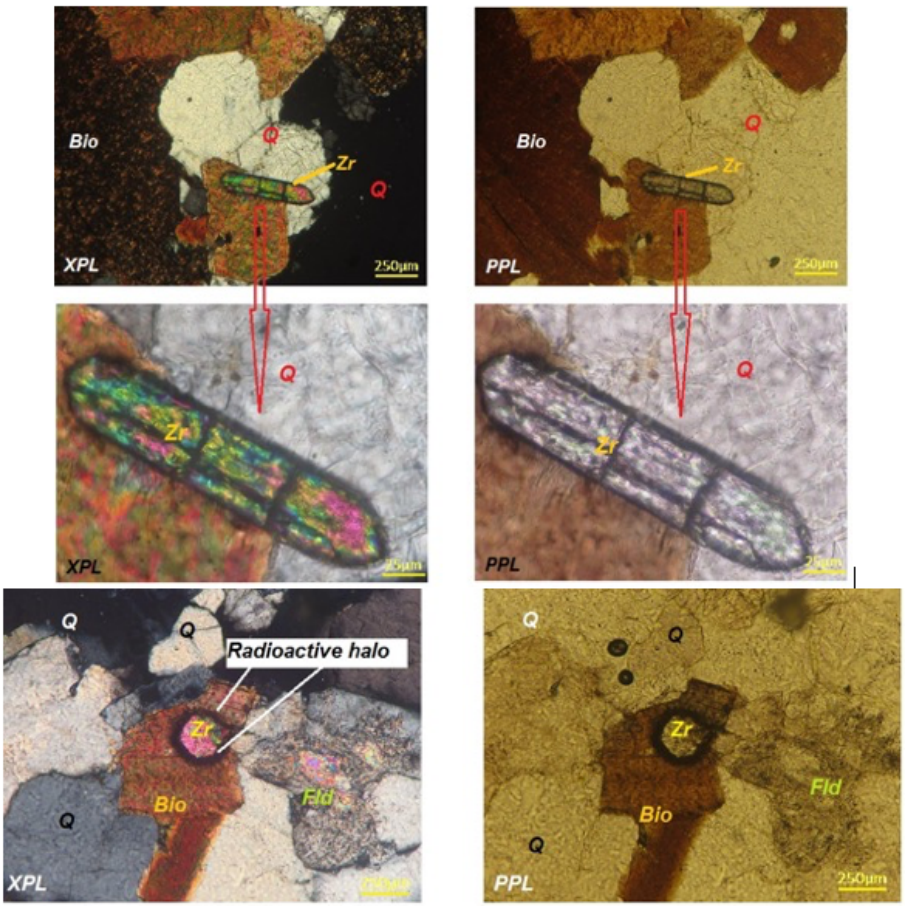

Figure 15 - Crystalline to semi-crystalline zircon as elliptical, prismatic, and halo inclusions in alkali feldspar, amphibole, and biotite

Sphene

Sphene is an abundant accessory mineral in igneous rocks and often appears in acidic plutonic and intermediate rocks as a titanite-rich mineral. Sphene is particularly abundant in granites and syenites.

Sphenes develop in semi-crystalline to crystalline forms inside local biotites. This mineral occurs more commonly than other titanite-rich minerals in the area, and no trace of its primary type was found in the Shirkuh granite (Fig. 16).

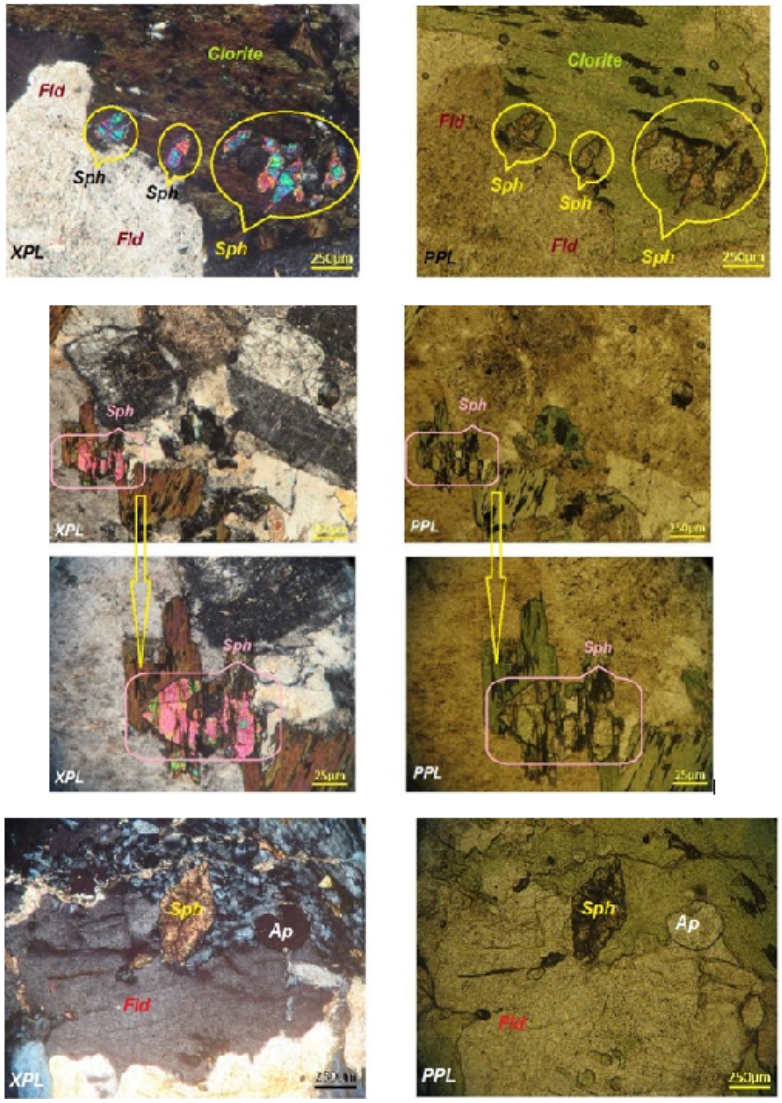

Figure 16 - Crystalline to amorphous titanite (sphene) in independent and inclusion forms in the plagioclase

Apatite

The apatite can originate most importantly in carbonates and alkaline igneous complexes. In pegmatites and granites (mostly alkali granites), apatite occurs in the form of veins (DANA, 1985). The apatite in local granites is often in the form of drawn, acicular, or hexagonal prisms, housed in plagioclase, amphibole, and alkali feldspars as inclusions occupying a small volume. The average size of the apatite grains is less than 1 mm. Apatite is one of the minerals that form in the final stages of solidification (Fig. 17).

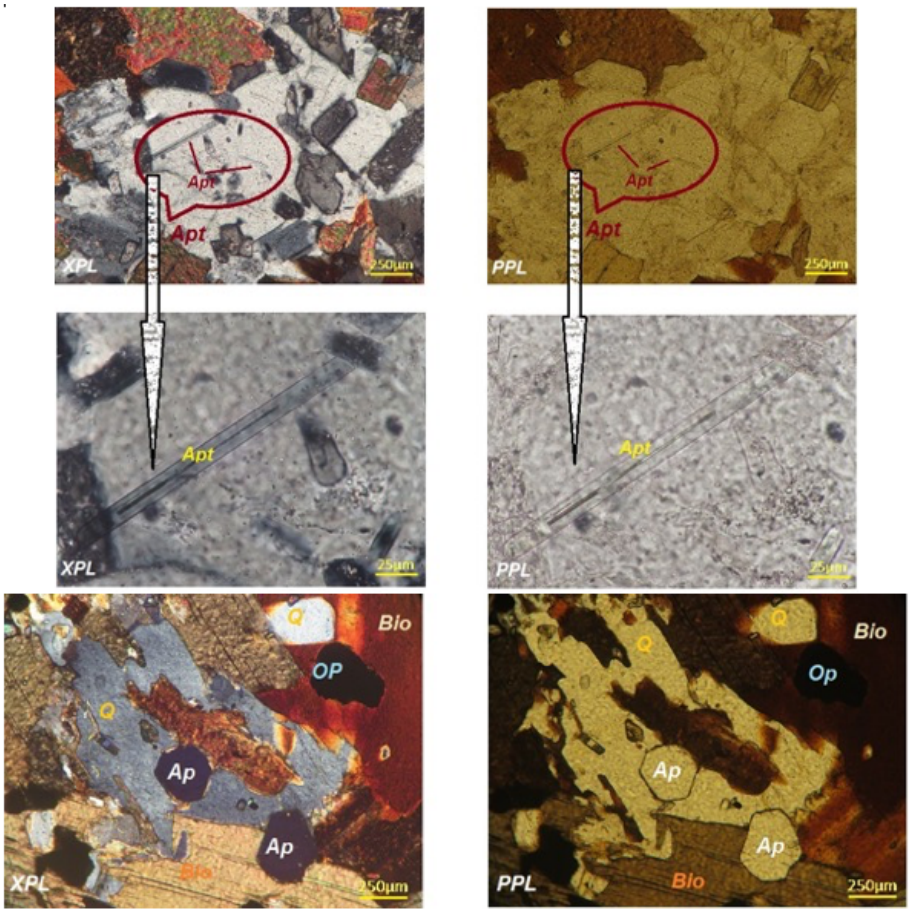

Figure 17 - Drawn hexagonal apatite prisms as inclusions in alkali feldspar and plagioclase

CONCLUSION

The most notable accessory minerals identified in the Shirkuh granite mass include garnet, tourmaline, amphibole, zircon, sphene, and apatite.

Based on its accessory minerals, these magmatic granites may be of the I- or S-types. Biotite and sphene are major I-type accessory minerals, and garnet and tourmaline are major S-type minerals.

Both uvarovite and grossular chromium-rich garnets can be found in the area. Laboratory studies on the parent granite rock showed the garnets have a considerable chromium content, which serves as evidence for the igneous origin of the garnets that crystallized directly from the granitic melt. Moreover, the lack of distinctive zoning in the garnet can show that the mineral is not of a metasomatic origin.

The investigations revealed the magmatic nature of the tourmaline found in the study region as the mineral had a higher iron content than magnesium, lacks strict zoning, and has formed in a closed magmatic system.

Radioactive elements accompany accessory minerals in granitoid masses. The minerals are significant in terms of geochemistry.

Acknowledgments

The authors would like to express their sincere gratitude to Dr. Afshin Ashja for his assistance with this study.

REFERÊNCIAS

HAJMOLLA ALI, A. **Geological map of Khezrabad 1:100000, Sreies sheet 6753.** Geological survey of Iran, Tehran (in Persion), 1993.

HAJMOLLA ALI, A.; MAJIDIFAR M.R. **Geological map of Yazd 1:100000.** Geological survey of Iran, Tehran (in Persion), 2000.

KHODAMI, M.; KAMALI SHERVEDANI, A. Mineralogical and geochemical characteristics of the Chah-Shur clay deposit, Southeast of Isfahan, Iran, **Iranian Journal of Earth Sciences**, 10(2), p. 135-141, 2018.

MOBASHERGARMI, M.; ZARAISAHAMIA, R.; AGHAZADEH, M.; AHMADIKHALAJI, A.; AHMADZADEH, GH. Mineral chemistry and thermobarometry of Eocene alkaline volcanic rocks in SW Germi, NW Iran, **Iranian Journal of Earth Sciences** 10 (1), p. 39-51, 2018.

NOVRUZOV, N.; VALIYEV, A.; BAYRAMOV, A.; MAMMADOV, S.; IBRAHIMOV, J.; EBDULREHIMLI, A. Mineral composition and paragenesis of altered and mineralized zones in the Gadir low sulfidation epithermal deposit (Lesser Caucasus, Azerbaijan), **Iranian Journal of Earth Sciences**, 11(1), p. 14-29, 2019.

YAZDI, A.; ASHJA-ARDALAN, A.; EMAMI, M.H.; DABIRI, R.; FOUDAZI, M. Chemistry of Minerals and Geothermobarometry of Volcanic Rocks in the Region Located in Southeast of Bam, Kerman Province. **Open Journal of Geology**, 7, p. 1644-1653, 2017.

YAZDI, A.; ASHJA-ARDALAN, A.; EMAMI, M.H.; DABIRI, R.; FOUDAZI, M. Magmatic interactions as recorded in plagioclase phenocrysts of quaternary volcanics in SE Bam (SE Iran). **Iranian Journal of Earth Sciences**, 11(3), p. 215-224, 2019.